MIMO Robust Disturbance Feedback Control for Refrigeration Systems Via an LMI Approach

Kawai, Fukiko; Vinther, Kasper; Andersen, Palle; Bendtsen, Jan Dimon

Published in:
IFAC-PapersOnLine

DOI (link to publication from Publisher):
10.1016/j.ifacol.2017.08.2075

Publication date:
2017

Document Version
Publisher's PDF, also known as Version of record

Available online at www.sciencedirect.com

ScienceDirect

IFAC Papers Online CONFERENCE PAPER ARCHIVE

IFAC PapersOnLine 50-1 (2017) 14525–14532

MIMO Robust Disturbance Feedback Control for Refrigeration Systems via an LMI Approach

Fukiko Kawai * ,** **Kasper Vinther** ** **Palle Andersen** **
Jan D. Bendtsen **

* *Fuji Electric Co., Ltd., Tokyo, Japan. (e-mail: kawai-fukiko@fujielectric.com)*
** *Aalborg University, 9220 Aalborg, Denmark (e-mail: fukiko, kv, pa, dimon@es.aau.dk)*

Abstract: This paper proposes Multi Input and Multi Output (MIMO) robust Disturbance Feedback Control (DFC) design using Linear Matrix Inequalities (LMIs). DFC can be added to existing controllers as an additional control loop, to attenuate disturbances and model uncertainties. The extended state space representation of the overall system is considered with parametric model uncertainties. LMIs are formulated to solve the optimization problem such that the DFC satisfies Lyapunov stability and robust performance. DFC was applied in the superheat control and the suction pressure control for a refrigeration system, and experimental results shows that DFC improves disturbance rejection compared to conventional PI controllers.

Keywords: Disturbance rejection, PID control, Robust control, Uncertain linear systems.

1. INTRODUCTION

PID control has been widely adopted in industrial control systems due to its simplicity and low cost, e.g., see Åström and Hägglund (2005). Conventional PID control has only been designed for Single-input and Single-output (SISO) systems , and the design is typically based on a linear time invariant (LTI) system description without model uncertainties, which means the classical PID controllers do not consider the modeling error and mutual interactions for Multi-input and Multi-output (MIMO) systems explicitly.

Robust control design is a method to guarantee stability and performance of systems with model uncertainty. In addition, the robust control design can be extended easily to MIMO control systems using state-space representation. Therefore, the robust control design method can be a powerful tool to address the issue of the conventional PID control. Moreover, the robust control design can be formulated using LMIs as Semi Definite Programming (SDP), and the SDP can be solved systematically with an optimization solver such as CVX by Michael Grant and Stephen Boyd (2014).

Many researchers have proposed robust PID control or low order robust controllers, for satisfying stability and robustness of systems, e.g., see Sivrioglu and Nonami (1996), Ge et al. (2002), Sadabadi and Karimi (2013). As for MIMO design, MIMO PID tuning by an iterative LMI procedure has been proposed as a new challenge by Boyd et al. (2015).

The authors of this paper suggests to improve the existing control in closed-loop systems using Disturbance Feedback Control (DFC) as shown in Fig. 1. We have proposed simple grid-based DFC design using robust control theory

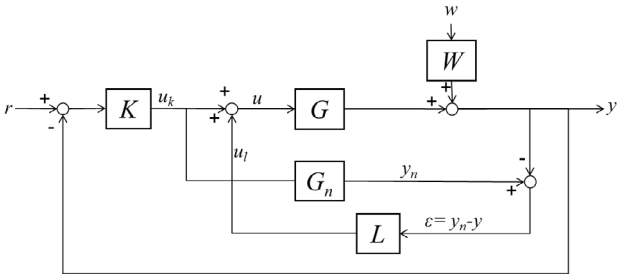

Fig. 1. Block diagrams of disturbance feedback control.

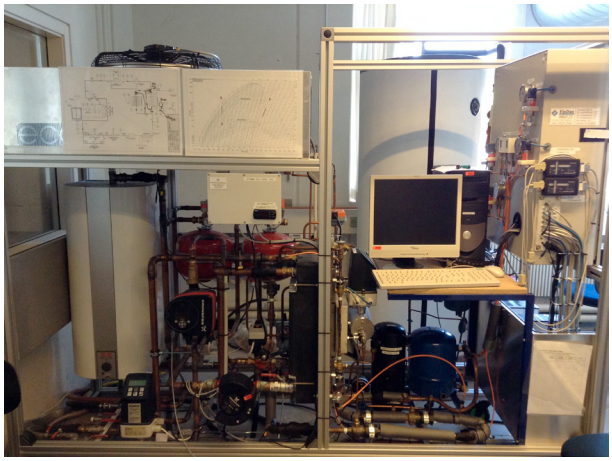

Fig. 2. The refrigeration system test setup at Aalborg University.

for industrial control devices such as Programmable Logic Controllers (PLCs), for more detail see Kawai et al. (2015). This method is for SISO systems, and it could be improved

2405-8963
Peer review under responsibility of International Federation of Automatic Control.
10.1016/j.ifacol.2017.08.2075

if the DFC applies systematic design methods using LMIs for MIMO systems.

One of the industrial companies in Japan, Fuji Electric has applied control to V/f (motor voltage/output frequency) using a similar control structure, which is called "disturbance observer" proposed by Ohnishi Ohishi et al. (1983), to compensate for the dead-time voltage error (Hoshino et al. (2007)). This design method has important issues to guarantee the robustness for variation of the motor parameters.

For these reasons, this paper presents a robust design method for the same DFC using LMIs for MIMO systems with model uncertainty. DFC is applied in the superheat control and the suction pressure control for the refrigeration system, and the effectiveness against the heat load disturbances using PI with/without DFC is examined.

The rest of the paper first describes the problem definition and the parametric uncertainty model in Section 2. Next, Section 3 then shows the LMIs formulations for DFC design. After that, practical examples are demonstrated in Section 4 using the refrigeration system as shown in Fig. 2. Finally, discussion and conclusions are described in Section 5.

2. PROBLEM DEFINITION

Fig. 1 shows a block diagram of a closed-loop system with DFC (L block), where r is the reference input, $u = u_k + u_l$ is the control input, y is the plant output, w is the disturbance, W is a weighting function, G is the plant, G_n is the nominal plant model, K is an existing feedback controller, L is the transfer function of the disturbance feedback, y_n is the output of the nominal plant, and ϵ is the error between y_n and y. The block diagram indicates that the DFC compensates for the disturbance using u_l. Furthermore, DFC does not add anything to the control input if the plant has no model uncertainty, or disturbance. Therefore, the basic features and performance of the existing system can be maintained with DFC. For this reason, the proposed method is an effective technique to handle disturbances and model uncertainty for various systems. Note that, although superficially similar, this configuration is not identical to model reference control.

2.1 Design Concepts for Disturbance Feedback Control

Fig. 3 shows a general closed-loop system with two input, two output formulation (left) and the closed-loop system for DFC $L(s)$ (Right). In general, when designing controllers, the transfer function T from w to z, where z is the output for evaluating the performance of the controlled systems and y are the measurements.

Note that the motivation of the DFC design is to improve the existing system. We assume that the existing controller K is fixed, meaning we can deal with K as a part of the plant P. Thus, P includes G, G_n, W, and K in the DFC design.

2.2 Parametric Uncertainty Model

Fig. 4 shows a block diagram of the closed-loop system with the addition of DFC. The plant model is transformed

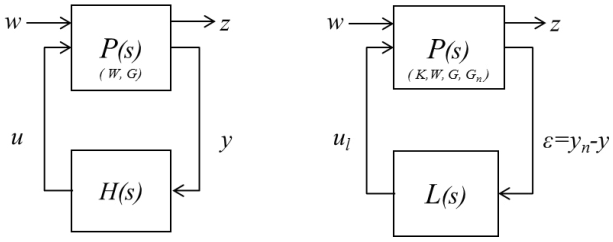

Fig. 3. A closed-loop system for design of an H_∞ controller $H(s)$ (Left), and a closed-loop system for design of Disturbance Feedback Control $L(s)$ (Right).

from the s-domain shown in Fig. 1 to a time domain representation;

$$\begin{aligned} \dot{\boldsymbol{x}} &= \boldsymbol{A}\boldsymbol{x} + \boldsymbol{B}\boldsymbol{u} \\ \boldsymbol{y} &= \boldsymbol{C}\boldsymbol{x}, \end{aligned} \tag{1}$$

where $\boldsymbol{A} \in \mathbb{R}^{n\times n}$, $\boldsymbol{B} \in \mathbb{R}^{n\times m}$, $\boldsymbol{C} \in \mathbb{R}^{m\times n}$.We assume that the plant model has no direct feed through $\boldsymbol{D}$ because most real thermo dynamical systems have relative degree at least one. The plant parameters are affected by parametric uncertainties (Carsten Scherer and Siep Weiland (2004)) expressed by

$$\boldsymbol{A} = \boldsymbol{A_n} + \sum_{i=1}^{p} \delta_{a,i}\boldsymbol{A_i}, \quad \delta_{a,i} \in [-1, +1], \tag{2}$$

$$\boldsymbol{B} = \boldsymbol{B_n} + \sum_{i=1}^{q} \delta_{b,i}\boldsymbol{B_i}, \quad \delta_{b,i} \in [-1, +1], \tag{3}$$

$$\boldsymbol{C} = \boldsymbol{C_n} + \sum_{i=1}^{r} \delta_{c,i}\boldsymbol{C_i}, \quad \delta_{c,i} \in [-1, +1], \tag{4}$$

where $\boldsymbol{\delta_a} = (\delta_{a,i}, \ldots, \delta_{a,p})$, $\boldsymbol{\delta_b} = (\delta_{b,i}, \ldots, \delta_{b,q})$, $\boldsymbol{\delta_c} = (\delta_{c,i}, \ldots, \delta_{c,r})$ are unknown vectors, which express the ensemble of all uncertainty quantities in a given dynamics and $\boldsymbol{A_n}$, $\boldsymbol{B_n}$, and $\boldsymbol{C_n}$ are the nominal state space representation using G_n and $\boldsymbol{A_i}$, $\boldsymbol{B_i}$, and $\boldsymbol{C_i}$ describe the uncertainty.

2.3 PI Controller

We consider PI controllers as the existing controller $\boldsymbol{K}$;

$$\begin{aligned} \dot{\boldsymbol{x}}_{\boldsymbol{k}} &= \boldsymbol{A_k}\boldsymbol{x_k} + \boldsymbol{B_k}(\boldsymbol{r} - \boldsymbol{y}), \\ \boldsymbol{u_k} &= \boldsymbol{C_k}\boldsymbol{x_k} + \boldsymbol{D_k}(\boldsymbol{r} - \boldsymbol{y}), \end{aligned} \tag{5}$$

where $\boldsymbol{A_k} \in \mathbb{R}^{m\times m}$, $\boldsymbol{B_k} \in \mathbb{R}^{m\times m}$, $\boldsymbol{C_k} \in \mathbb{R}^{m\times m}$, and $\boldsymbol{D_k} \in \mathbb{R}^{m\times m}$ are the state space representation of $\boldsymbol{K}$. If SISO system with a PI controller is considered, then $A_k = 0, B_k = 1, C_k = k_i$, and $D_k = k_p$, where k_p is a proportional gain, and k_i is an integral gain.

2.4 Disturbance Weighting Function

We consider a disturbance weighting function. The weighting function for the disturbance $\boldsymbol{w}$ is defined as

$$\begin{aligned} \dot{\boldsymbol{x}}_{\boldsymbol{w}} &= \boldsymbol{A_w}\boldsymbol{x_w} + \boldsymbol{B_w}\boldsymbol{w}, \\ \boldsymbol{y_w} &= \boldsymbol{C_w}\boldsymbol{x_w} + \boldsymbol{D_w}\boldsymbol{w}, \end{aligned} \tag{6}$$

where $\boldsymbol{A_w} \in \mathbb{R}^{m_w\times m_w}$, $\boldsymbol{B_w} \in \mathbb{R}^{m_w\times m_w}$, $\boldsymbol{C_w} \in \mathbb{R}^{m_w\times m_w}$, and $\boldsymbol{D_w} \in \mathbb{R}^{m_w\times m_w}$ are the state space representation of the weighting function. Note that this choice of order s may depend on the given application. Here, we simply chose $m_w = m$

2.5 Disturbance Feedback Controller

The Disturbance Feedback Controller (DFC) is chosen as

$$\begin{aligned} \dot{\boldsymbol{x}}_{\boldsymbol{ul}} &= \boldsymbol{A_l x_{ul}} + \boldsymbol{B_l \epsilon} \\ \boldsymbol{u_l} &= \boldsymbol{C_l x_{ul}} + \boldsymbol{D_l \epsilon}, \end{aligned} \tag{7}$$

where $\boldsymbol{A_l} \in \mathbb{R}^{2n+m+m_w \times 2n+m+m_w}$, $\boldsymbol{B_l} \in \mathbb{R}^{2n+m+m_w \times m}$, $\boldsymbol{C_l} \in \mathbb{R}^{m \times 2n+m+m_w}$, and $\boldsymbol{D_l} \in \mathbb{R}^{m \times m}$ are the state space representation of the DFC. Note that the DFC is defined as full order controller because the dimension of the plant P in Fig. 3 is $dim(G)+dim(G_n)+dim(K)+dim(W) = n+n+m+m_w$.

3. LMI FORMULATION FOR DFC DESIGN

In this section, we present a MIMO robust DFC design method based on output feedback control via an LMI approach. Firstly, the closed loop system $T(s)$ is obtained by the extended state space representation. Next, two constraints are introduced to design DFC. Here, we make use of the Bounded Real Lemma and regional pole placement for continuous time systems Scherer et al. (1997). The Bounded Real Lemma is used to guarantee a robust performance, and regional pole placement is introduced to specify the control performance. Moreover, a linearizing change of variables is introduced to design DFC. The DFC is categorized as an output feedback control. Therefore, a linearizing change of variable is needed to formulate the problem in terms of LMI.

3.1 The Extended State Space Representation

If the setpoint $r = 0$, the extended state space representation of the overall system in Fig. 4 can be written as follows;

$$\begin{aligned} \dot{\boldsymbol{x_p}} &= \boldsymbol{A_p x_p} + \boldsymbol{B_{w1} w} + \boldsymbol{B_p u_l} \\ \boldsymbol{z} &= \boldsymbol{C_z x_p} + \boldsymbol{D_z u_l} \\ \boldsymbol{\epsilon} &= \boldsymbol{C_p x_p} + \boldsymbol{D_{w1} w}, \end{aligned} \tag{8}$$

where

$$\boldsymbol{x_p} = \left(\boldsymbol{x}\ \boldsymbol{x_n}\ \boldsymbol{x_k}\ \boldsymbol{x_w} \right)^{\mathrm{T}},$$

$$\boldsymbol{A_p} = \begin{pmatrix} \boldsymbol{A - BD_kC} & \boldsymbol{0} & \boldsymbol{BC_k} & \boldsymbol{-BD_kC_w} \\ \boldsymbol{-B_nD_kC} & \boldsymbol{A_n} & \boldsymbol{B_nC_k} & \boldsymbol{-B_nD_kC_w} \\ \boldsymbol{-B_kC} & \boldsymbol{0} & \boldsymbol{A_k} & \boldsymbol{-B_kC_w} \\ \boldsymbol{0} & \boldsymbol{0} & \boldsymbol{0} & \boldsymbol{A_w} \end{pmatrix},$$

$$\boldsymbol{B_{w1}} = \left(\begin{array}{cccc} \boldsymbol{0} & \boldsymbol{0} & \boldsymbol{0} & \boldsymbol{0} \\ \hline \boldsymbol{-BD_w} & \boldsymbol{-B_nD_w} & \boldsymbol{-B_kD_w} & \boldsymbol{B_w} \end{array} \right)^{\mathrm{T}},$$

$$\boldsymbol{B_p} = \left(\boldsymbol{B}\ \boldsymbol{0}\ \boldsymbol{0}\ \boldsymbol{0} \right)^{\mathrm{T}},$$

$$\boldsymbol{C_z} = \left(\begin{array}{cccc} \boldsymbol{-C} & \boldsymbol{C_n} & \boldsymbol{0} & \boldsymbol{-C_w} \\ \hline \boldsymbol{0} & \boldsymbol{0} & \boldsymbol{0} & \boldsymbol{0} \end{array} \right),$$

$$\boldsymbol{C_p} = \left(\boldsymbol{-C}\ \boldsymbol{C_n}\ \boldsymbol{0}\ \boldsymbol{-C_w} \right),$$

$$\boldsymbol{D_z} = \left(\begin{array}{c} \boldsymbol{0} \\ \hline \boldsymbol{\rho_z I} \end{array} \right), \quad \boldsymbol{D_{w1}} = \left(\boldsymbol{\rho_w I} \middle| \boldsymbol{0} \right),$$

w is an output disturbance, and ρ_z and ρ_w are a small numbers which are introduced to maintain full rank and to avoid numerical issues if $\boldsymbol{D_z}$ and $\boldsymbol{D_{w1}}$ are zero matrices.

The closed loop transfer function $T(s)$ from $\boldsymbol{w}$ to $\boldsymbol{z}$ is defined as follows;

$$\begin{aligned} \dot{\boldsymbol{x_{cl}}} &= \boldsymbol{\mathcal{A} x_{cl}} + \boldsymbol{\mathcal{B} w} \\ \boldsymbol{z} &= \boldsymbol{\mathcal{C} x_{cl}} + \boldsymbol{\mathcal{D} w}, \end{aligned} \tag{9}$$

where

$$\left(\begin{array}{c|c} \boldsymbol{\mathcal{A}} & \boldsymbol{\mathcal{B}} \\ \hline \boldsymbol{\mathcal{C}} & \boldsymbol{\mathcal{D}}, \end{array} \right) =$$

$$\left(\begin{array}{cc|c} \boldsymbol{A_p + B_pD_lC_p} & \boldsymbol{B_pC_l} & \boldsymbol{B_{w1} + B_pD_lD_{w1}} \\ \boldsymbol{B_lC_p} & \boldsymbol{A_l} & \boldsymbol{B_lD_{w1}} \\ \hline \boldsymbol{C_z + D_zD_lC_p} & \boldsymbol{D_zC_l} & \boldsymbol{D_zD_lD_{w1}} \end{array} \right).$$

Note that $\boldsymbol{z} = (\boldsymbol{\epsilon_z}, \boldsymbol{D_z u_l})^{\mathrm{T}}$ is defined in order to distinguish each performance, where $\boldsymbol{\epsilon_z} = \boldsymbol{y_n} - (\boldsymbol{y} - \boldsymbol{D_w w})$, and $\boldsymbol{\epsilon_z}$ is defined without the direct-thorough of disturbance $\boldsymbol{D_w w}$.

3.2 Bounded Real Lemma

The Bounded Real Lemma is used for the constraints in the DFC design. $\boldsymbol{\mathcal{A}}$ is stable and the H_∞ norm of $T(s)$ is smaller than γ if and only if there exists a Lyapunov matrix $\boldsymbol{\mathcal{P}}$, which satisfies the following two lemmas (Gahinet and Apkarian (1994); Cottle (1974)).

Lemma1: *The LMI*

$$\begin{pmatrix} \boldsymbol{Q(x)} & \boldsymbol{S(x)} \\ \boldsymbol{S(x)} & \boldsymbol{R(x)} \end{pmatrix} > 0, \tag{10}$$

where $\boldsymbol{Q(x)} = \boldsymbol{Q(x)}^{\mathrm{T}}$, $\boldsymbol{R(x)} = \boldsymbol{R(x)}^{\mathrm{T}}$, *and* $\boldsymbol{S(x)}$ *depend affinely on x, is equivalent to*

$$\boldsymbol{R(x)} > 0, \tag{11}$$

$$\boldsymbol{Q(x) - S(x)R(x)^{-1}S(x)}^{\mathrm{T}} > 0. \tag{12}$$

Lemma2: *Consider a continuous-time transfer function* $T(s)$ *of realizations* $T(s) = \boldsymbol{\mathcal{D} + \mathcal{C}(sI - \mathcal{A})^{-1}\mathcal{B}}$. *The following statements are equivalent:*

1. $\|\boldsymbol{\mathcal{D} + \mathcal{C}(sI - \mathcal{A})^{-1}\mathcal{B}}\|_\infty < \gamma$ (13)
   and $\boldsymbol{\mathcal{A}}$ *is stable in the continious-time sense* $(Re(\lambda_i(\boldsymbol{\mathcal{A}})) < 0)$.
2. *There exist a symmetric positive definite solution* $\boldsymbol{\mathcal{P}}$ *to the LMI:*

$$\begin{pmatrix} \boldsymbol{\mathcal{A}}^{\mathrm{T}}\boldsymbol{\mathcal{P}} + \boldsymbol{\mathcal{P}\mathcal{A}} & \boldsymbol{\mathcal{P}\mathcal{B}} & \boldsymbol{\mathcal{C}}^{\mathrm{T}} \\ \boldsymbol{\mathcal{B}}^{\mathrm{T}}\boldsymbol{\mathcal{P}} & \boldsymbol{-\gamma I} & \boldsymbol{\mathcal{D}}^{\mathrm{T}} \\ \boldsymbol{\mathcal{C}} & \boldsymbol{\mathcal{D}} & \boldsymbol{-\gamma I} \end{pmatrix} < 0. \tag{14}$$

3.3 Regional Pole Placement

The Regional Pole Placement is used to stabilize the control systems in the DFC design (Chilali et al. (1999)). The regional pole constraints is introduced with Theorem 1 as follows.

Theorem 1: The matrix $\boldsymbol{\mathcal{A}}$ has all its eigenvalues in the LMI region $\{z \in C : f_{\mathcal{D}}(z) < 0\}$ with $f_{\mathcal{D}} : \mathbb{C} \to \mathbb{R}$:

$$\begin{aligned} f_{\mathcal{D}}(z) &= \boldsymbol{\alpha} + z\boldsymbol{\beta} + \bar{z}\boldsymbol{\beta}^{\mathrm{T}} \\ &= [\alpha_{ij} + \beta_{ij}z + \beta_{ji}\bar{z}]_{1 \le i,j \le l}, \end{aligned} \tag{15}$$

where $\boldsymbol{\alpha} = [\alpha_{ij}] \in \mathbb{R}^{l \times l}$ and $\boldsymbol{\beta} = [\beta_{ij}] \in \mathbb{R}^{l \times l}$ are symmetric matrices, and if and only if there exists a symmetric Lyapunov matrix $\boldsymbol{\mathcal{P}}$ such that

$$[\alpha_{ij}\boldsymbol{\mathcal{P}} + \beta_{ij}\boldsymbol{\mathcal{A}}^{\mathrm{T}}\boldsymbol{\mathcal{P}} + \beta_{ji}\boldsymbol{\mathcal{P}\mathcal{A}}]_{i,j} < 0, \quad \boldsymbol{\mathcal{P}} > 0. \tag{16}$$

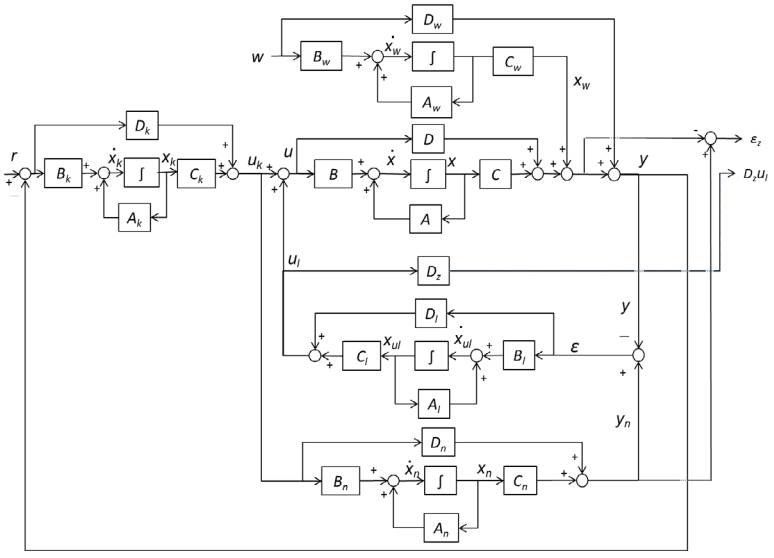

Fig. 4. State space representation of the DFC design.

Note that the left hand side of the first inequality in (15) is given in terms of the Kronecker product, which for any two matrices, e.g., $\boldsymbol{A}$ and $\boldsymbol{B}$, is defined as

$$\boldsymbol{A} \otimes \boldsymbol{B} = [\boldsymbol{A}_{ij}\boldsymbol{B}]_{ij}. \tag{17}$$

In addition, the function $f_{\mathcal{D}}$ takes values in the space of $l \times l$ Hermitian matrices.

3.4 Linearizing Change of Variables

As we described, DFC is categorized as an output-feedback case and a linearizing change of variables can therefore be used to design DFC. The Lyapunov matrix $\boldsymbol{\mathcal{P}}$ is partitioned, for more detail see Scherer et al. (1997), as follows;

$$\boldsymbol{\mathcal{P}} = \begin{pmatrix} \boldsymbol{Y} & \boldsymbol{N} \\ \boldsymbol{N}^{\mathrm{T}} & \star \end{pmatrix}, \boldsymbol{\mathcal{P}}^{-1} = \begin{pmatrix} \boldsymbol{X} & \boldsymbol{M} \\ \boldsymbol{M}^{\mathrm{T}} & \star \end{pmatrix}, \tag{18}$$

$$\boldsymbol{\mathcal{P}\Pi_1} = \boldsymbol{\Pi_2}, \tag{19}$$

where

$$\boldsymbol{\Pi_1} := \begin{pmatrix} \boldsymbol{X} & \boldsymbol{I} \\ \boldsymbol{M}^{\mathrm{T}} & \boldsymbol{0} \end{pmatrix}, \boldsymbol{\Pi_2} := \begin{pmatrix} \boldsymbol{I} & \boldsymbol{Y} \\ \boldsymbol{0} & \boldsymbol{N}^{\mathrm{T}} \end{pmatrix},$$

and $\boldsymbol{X}$ and $\boldsymbol{Y}$ are symmetric matrices. Then we define the change of the variables as follows;

$$\begin{aligned} \hat{\boldsymbol{A}} :=& \boldsymbol{N}\boldsymbol{A}_{\boldsymbol{l}}\boldsymbol{M}^{\mathrm{T}} + \boldsymbol{N}\boldsymbol{B}_{\boldsymbol{l}}\boldsymbol{C}_{\boldsymbol{p}}\boldsymbol{X} + \boldsymbol{Y}\boldsymbol{B}_{\boldsymbol{p}}\boldsymbol{C}_{\boldsymbol{l}}\boldsymbol{M}^{\mathrm{T}} \\ &+ \boldsymbol{Y}(\boldsymbol{A}_{\boldsymbol{p}} + \boldsymbol{B}_{\boldsymbol{p}}\boldsymbol{D}_{\boldsymbol{l}}\boldsymbol{C}_{\boldsymbol{p}})\boldsymbol{X}, \end{aligned} \tag{20}$$

$$\hat{\boldsymbol{B}} := \boldsymbol{N}\boldsymbol{B}_{\boldsymbol{l}} + \boldsymbol{Y}\boldsymbol{B}_{\boldsymbol{p}}\boldsymbol{D}_{\boldsymbol{l}}, \tag{21}$$

$$\hat{\boldsymbol{C}} := \boldsymbol{C}_{\boldsymbol{l}}\boldsymbol{M}^{\mathrm{T}} + \boldsymbol{D}_{\boldsymbol{l}}\boldsymbol{C}_{\boldsymbol{p}}\boldsymbol{X}, \tag{22}$$

$$\hat{\boldsymbol{D}} := \boldsymbol{D}_{\boldsymbol{l}}. \tag{23}$$

The LMI optimization finds $\hat{\boldsymbol{A}}, \hat{\boldsymbol{B}}, \hat{\boldsymbol{C}}, \hat{\boldsymbol{D}}, \boldsymbol{X}, \boldsymbol{Y}$ instead of $\boldsymbol{A_l}, \boldsymbol{B_l}, \boldsymbol{C_l}, \boldsymbol{D_l}$, and $\boldsymbol{\mathcal{P}}$. After that, the DFC is given by the results of the optimization problem;

$$\boldsymbol{D}_{\boldsymbol{l}} := \hat{\boldsymbol{D}}, \tag{24}$$

$$\boldsymbol{C}_{\boldsymbol{l}} := (\hat{\boldsymbol{C}} - \boldsymbol{D}_{\boldsymbol{l}}\boldsymbol{C}_{\boldsymbol{p}}\boldsymbol{X})\boldsymbol{M}^{-\mathrm{T}}, \tag{25}$$

$$\boldsymbol{B}_{\boldsymbol{l}} := \boldsymbol{N}^{-\boldsymbol{1}}(\hat{\boldsymbol{B}} - \boldsymbol{Y}\boldsymbol{B}_{\boldsymbol{p}}\boldsymbol{D}_{\boldsymbol{l}}), \tag{26}$$

$$\begin{aligned} \boldsymbol{A}_{\boldsymbol{l}} :=& \boldsymbol{N}^{-\boldsymbol{1}}(\hat{\boldsymbol{A}} - \boldsymbol{N}\boldsymbol{B}_{\boldsymbol{l}}\boldsymbol{C}_{\boldsymbol{p}}\boldsymbol{X} - \boldsymbol{Y}\boldsymbol{B}_{\boldsymbol{p}}\boldsymbol{C}_{\boldsymbol{l}}\boldsymbol{M}^{\mathrm{T}} \\ &- \boldsymbol{Y}(\boldsymbol{A}_{\boldsymbol{p}} + \boldsymbol{B}_{\boldsymbol{p}}\boldsymbol{D}_{\boldsymbol{l}}\boldsymbol{C}_{\boldsymbol{p}})\boldsymbol{X})\boldsymbol{M}^{-\mathrm{T}}. \end{aligned} \tag{27}$$

3.5 Optimization Problem for DFC Design

Now, we summarize the conditions, which are described in subsections 3.1 to 3.4. The optimization problem after the change of variables is given by

$$\text{minimize } \gamma, \tag{28}$$

$$\text{subject to;} \tag{29}$$

$$\begin{pmatrix} \hat{\boldsymbol{\mathcal{A}}}^{\mathrm{T}}\hat{\boldsymbol{\mathcal{P}}} + \hat{\boldsymbol{\mathcal{P}}}\hat{\boldsymbol{\mathcal{A}}} & \hat{\boldsymbol{\mathcal{P}}}\hat{\boldsymbol{\mathcal{B}}} & \hat{\boldsymbol{\mathcal{C}}}^{\mathrm{T}} \\ \hat{\boldsymbol{\mathcal{B}}}^{\mathrm{T}}\hat{\boldsymbol{\mathcal{P}}} & -\gamma\boldsymbol{I} & \hat{\boldsymbol{\mathcal{D}}}^{\mathrm{T}} \\ \hat{\boldsymbol{\mathcal{C}}} & \hat{\boldsymbol{\mathcal{D}}} & -\gamma\boldsymbol{I} \end{pmatrix} < 0, \quad \gamma > 0,$$

$$\hat{\boldsymbol{\mathcal{P}}} = \begin{pmatrix} \boldsymbol{X} & \boldsymbol{I} \\ \boldsymbol{I} & \boldsymbol{Y} \end{pmatrix}, \quad \hat{\boldsymbol{\mathcal{P}}} > 0,$$

$$[\alpha_{ij}\boldsymbol{\mathcal{P}} + \beta_{ij}\boldsymbol{\mathcal{A}}^{\mathrm{T}}\boldsymbol{P} + \beta_{ji}\boldsymbol{\mathcal{P}}\boldsymbol{\mathcal{A}}]_{i,j} < 0,$$

where

$$\hat{\boldsymbol{\mathcal{A}}}^{\mathrm{T}}\hat{\boldsymbol{\mathcal{P}}} + \hat{\boldsymbol{\mathcal{P}}}\hat{\boldsymbol{\mathcal{A}}} = \begin{pmatrix} \boldsymbol{A_p}\boldsymbol{X} + \boldsymbol{X}\boldsymbol{A_p}^{\mathrm{T}} + \boldsymbol{B_p}\hat{\boldsymbol{C}} + (\boldsymbol{B_p}\hat{\boldsymbol{C}})^{\mathrm{T}} & \hat{\boldsymbol{A}}^{\mathrm{T}} + (\boldsymbol{A_p} + \boldsymbol{B_p}\hat{\boldsymbol{D}}\boldsymbol{C_p})^{\mathrm{T}} \\ \hat{\boldsymbol{A}} + (\boldsymbol{A_p} + \boldsymbol{B_p}\hat{\boldsymbol{D}}\boldsymbol{C_p}) & \boldsymbol{A_p}^{\mathrm{T}}\boldsymbol{Y} + \boldsymbol{Y}\boldsymbol{A_p} + \hat{\boldsymbol{B}}\boldsymbol{C_p} + (\hat{\boldsymbol{B}}\boldsymbol{C_p})^{\mathrm{T}} \end{pmatrix},$$

$$\hat{\boldsymbol{\mathcal{P}}}\hat{\boldsymbol{\mathcal{B}}} = \begin{pmatrix} \boldsymbol{B_j} + \boldsymbol{B_p}\hat{\boldsymbol{D}}\boldsymbol{F_j} \\ \boldsymbol{Y}\boldsymbol{B_j} + \hat{\boldsymbol{B}}\boldsymbol{F_j} \end{pmatrix},$$

$$\hat{\boldsymbol{\mathcal{C}}} = \begin{pmatrix} \boldsymbol{C_j}\boldsymbol{X} + \boldsymbol{E_j}\hat{\boldsymbol{C}} & \boldsymbol{C_j} + \boldsymbol{E_j}\hat{\boldsymbol{D}}\boldsymbol{C_p} \end{pmatrix},$$

$$\hat{\boldsymbol{\mathcal{D}}} = \boldsymbol{E_j}\hat{\boldsymbol{D}}\boldsymbol{F_j},$$

$$\boldsymbol{B_j} := \boldsymbol{B_w}\boldsymbol{R_j}, \quad \boldsymbol{C_j} := \boldsymbol{L_j}\boldsymbol{C_z},$$

$$\boldsymbol{E_j} := \boldsymbol{L_j}\boldsymbol{D_z}, \quad \boldsymbol{F_j} := \boldsymbol{D_w}\boldsymbol{R_j},$$

and $\boldsymbol{L_j}, \boldsymbol{R_j}$ are input/output channel for $T(s)$ from $\boldsymbol{w}$ to $\boldsymbol{z}$;

$$\boldsymbol{T_j} = \boldsymbol{L_j}\boldsymbol{T}\boldsymbol{R_j}. \tag{30}$$

4. PRACTICAL EXAMPLE

4.1 Refrigeration System

The system includes four main components; a compressor, a condenser, an expansion valve, and an evaporator. In a

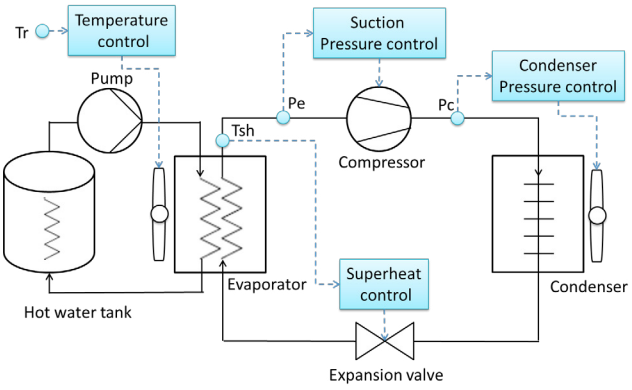

Fig. 5. A layout of the refrigeration system with basic control structure.

basic refrigeration system, one control device is installed for each component as shown in Fig. 5. These controllers regulate pressure or temperature based on operating conditions. A hot water tank is set as heat load. For example, the rotational speed of the compressor is controlled to keep a constant refrigerant suction pressure P_e. The opening degree of the expansion valve maintains a suitable refrigerant superheat T_{sh} (difference between the temperature at the outlet of the evaporator and the evaporation temperature inside the evaporator). The speed of the evaporator fan is controlled to keep the temperature on the load side T_r constant. The speed of the condenser fan is controlled in order to keep the condensing pressure P_c constant.

4.2 Modeling

Now 2 input and 2 output modeling for MIMO control design is considered. A simple superheat model and a suction pressure model is chosen for the MIMO control design and these models can be described by a first order plus dead time system, e.g., see Izadi-Zamanabadi et al. (2012). The model is created using experimental data obtained from step response tests conducted at different operating conditions.

$$\mathcal{G}_{ij} = \frac{k_{ij}}{1+\tau_{ij}s}e^{-\theta_{ij}s}; \tag{31}$$
$$k_{ij} \in [k_{min,ij}, k_{max,ij}], \tau_{ij} \in [\tau_{min,ij}, \tau_{max,ij}],$$
$$\theta_{ij} \in [\theta_{min,ij}, \theta_{max,ij}],$$
$$i = 1,2, j = 1,2.$$

Next, the nominal model is computed using average parameter values of $\mathcal{G}$.

$$G_{n,ij} = \frac{k_{n,ij}}{1+\tau_{n,ij}s}e^{-\theta_{n,ij}s}. \tag{32}$$

The data for estimation was sampled by the open loop step up/down responses. These tests were repeated twice for two conditions, one for low refrigerant flow and low load conditions, and one for high refrigerant flow and high load conditions. In all modeling situations, the condenser pressure is fixed at 9 bar as shown in Table 1.

Fig. 6 shows the input and output data, where operating point values are subtracted, and the data is analyzed for parameter estimation of the superheat control. Input data is OD, and output data is superheat.

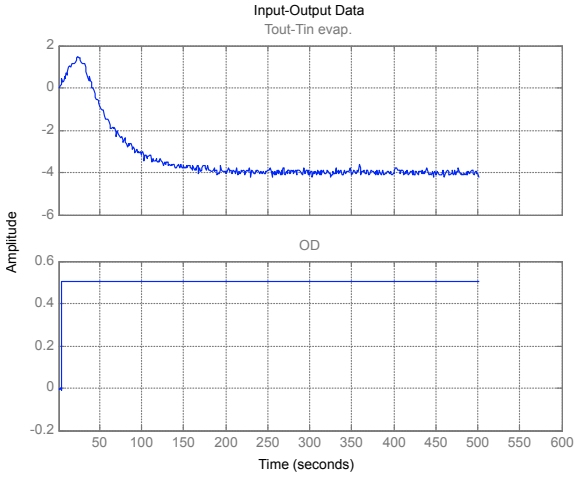

Fig. 6. Input-output data for superheat control design.

Fig. 7 shows comparison of the estimation results and real data for subsystem g_{11} using the Matlab system identification toolbox. The fitness was 85.01 %. The other subsystems were estimated by the same procedures, and finally the parameter space for the MIMO system is obtained as shown in Table 2.

For more simple DFC design, the time delay is approximated by a first order system. In addition, only one parameter k_{11} is chosen as main uncertainty because a plant gain of the superheat k_{11} is the most dominant part of the uncertainty and nonlinearity, shown in Table 2. Therefore, G and G_n are approximated as follows:

$$\mathcal{G}_{11} = \frac{k_{11}}{(1+\tau_{n,11}s)(1+\theta_{n,11}s)}; \tag{33}$$
$$k_{11} \in [k_{min,11}, k_{max,11}],$$

and the rest of the subsystems are expressed by the nominal model.

$$\mathcal{G}_{ij} = \frac{k_{n,ij}}{(1+\tau_{n,ij}s)(1+\theta_{n,ij}s)}; \tag{34}$$
$$i = 1,2, j = 1,2, except \;\; ij = 11.$$

These parameter values are shown in Table 3.

4.3 Tuning parameters

The PI controllers are designed using the parameters of each corner point of the $\mathcal{G}$ space to maintain the nominal stability.

Table 1. Modeling conditions.

Set point	Condition 1	Condition 2	PI or fixed
Superheat	10.0 [C]	10.0 [C]	PI
Compressor speed	40 [Hz]	50 [Hz]	fixed
Condenser pressure	9.0 [bar]	9.0 [bar]	PI
Water tank	14.0 [C]	16.0 [C]	PI

Table 2. Estimation results of parameter uncertainty corresponding to $-1 < \delta < 1$.

	k	τ	θ
g_{11}	[-10.65 -8.72]	[29.48 60.19]	[14 27]
g_{21}	[0.097 0.47]	[6.38 14.26]	[0 11]
g_{12}	[0.72 0.77]	[21.77 62.30]	[10 27]
g_{22}	[-0.071 -0.021]	[9.18 5.23]	[0 8]

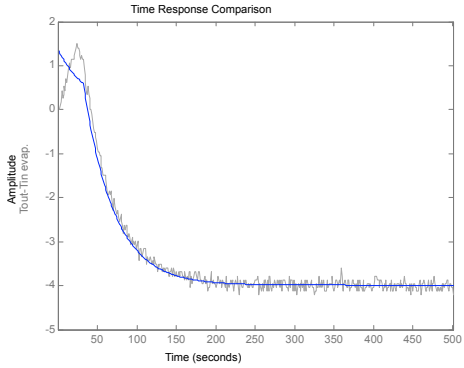

Fig. 7. Plots of the parameter estimation and real data.

$$\boldsymbol{K} = \begin{pmatrix} K_{11} & 0 \\ 0 & K_{22} \end{pmatrix}, \tag{35}$$

$$\textit{where} \quad K_{11} = \frac{\tau_{11min}}{1.52 k_{11min} \theta_{11max}}(1 + \frac{1}{\tau_{11min} s}),$$
$$K_{22} = \frac{\tau_{22min}}{2.50 k_{22min} \theta_{22max}}(1 + \frac{1}{\tau_{22min} s}).$$

Note that the plant gain k_{11} and k_{22} have negative sign, thus we should chose *minimum* value as the worst case.

The disturbance weight function is chosen as a first order system, and designed by the nominal time constant $\tau_{n,11}, \tau_{n,22}$. In addition, the weight of superheat W_{11} is given a priority for a disturbance rejection.

$$\boldsymbol{W} = \begin{pmatrix} W_{11} & 0 \\ 0 & W_{22} \end{pmatrix}. \tag{36}$$

$$\textit{where} \quad W_{11} = \frac{1}{1 + \frac{\tau_{n,11}}{3} s}, \; W_{22} = \frac{0.1}{1 + \tau_{n,22} s}.$$

The artificial parameters in (8) for DFC are chosen as follows:

$$\rho_z = 10^{-1}, \quad \rho_w = 10^{-6}. \tag{37}$$

4.4 DFC Design

The optimal H_∞ performance was $\gamma = 0.3940$ with full order DFC, and the DFC was a 20th order system because $A_l = 2n + m + m_w, n = 8, m = 2, m_w = 2$. It could be more useful for industrial applications if a lower order DFC can be obtained. For this reason, model reduction of DFC is considered, and the DFC gain $\boldsymbol{L}$ is obtained with the Matlab command `modred`.

$$\boldsymbol{L} = \begin{pmatrix} -0.3492 & 0.5071 \\ 1.393 & -6.533 \end{pmatrix}. \tag{38}$$

Fig. 8 shows a comparison of DFCs before/after the model reduction. The figure indicates that the DFC gain can keep the main feature of the original DFC in the low frequency area. Table 4 and Fig. 9 to Fig. 11 show the simulation

Table 3. Primary parameter uncertainty and nominal parameters for LMI design.

	k	τ	θ
g_{11}	[-10.65 -8.72]	[44.84]	[20.50]
$g_{n,21}$	[0.29]	[10.32]	[5.50]
$g_{n,12}$	[0.75]	[42.03]	[18.50]
$g_{n,22}$	[-0.046]	[7.21]	[4.00]

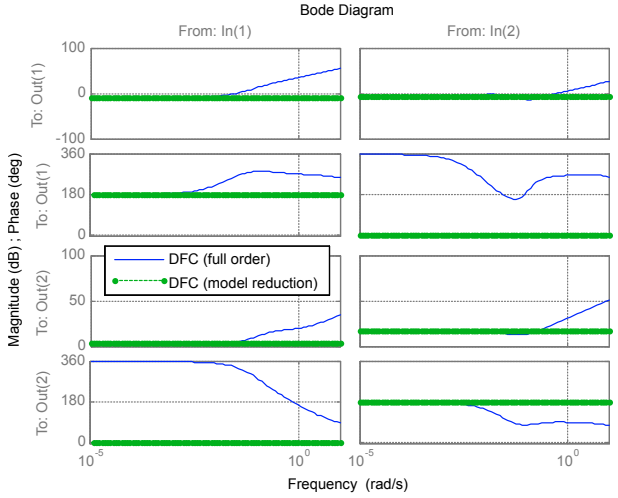

Fig. 8. Bode plots of DFC from ϵ to u_l, before and after model reduction.

results for comparing PI control with full order DFC or DFC gain. The set-point and disturbance were changed for the superheat control. These results indicate that DFC gain can improve the disturbance rejection more than 40 %. In addition, the DFC gain shows robustness against model uncertainties for the step response simulation as well as full order DFC. From these results, we can choose the DFC gain instead of the full order DFC.

Table 4. IAE of the simulation results.

	PI	PI + DFC (full order)	PI + DFC (gain)
The superheat control	464.76	260.00	263.67
The suction pressure control	8.97	11.94	14.94

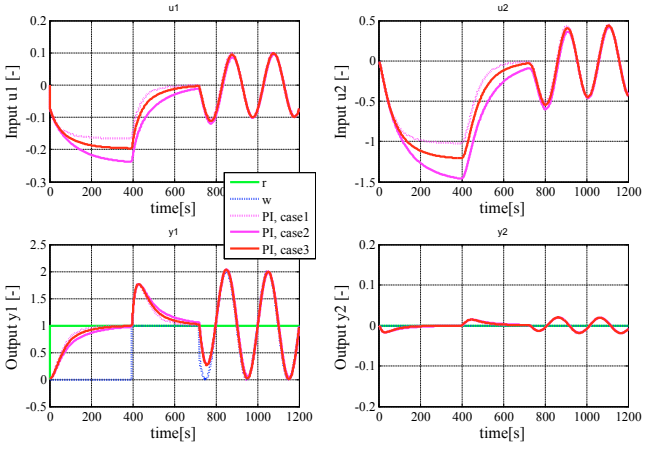

Fig. 9. Simulation results using PI control without DFC.

4.5 Experimental Results

Table 5 shows the experimental condition for each component. Each set point follows the modeling condition in section 4.2 to examine the $\mathcal{G}$ space. Superheat control and suction pressure control are examined by PI with/without DFC for MIMO control systems. The temperature of the water tank is set at 14 degree for the initial condition. Then the set point is changed to 13.5 degree, and kept there for the first 500 seconds for making swing load disturbance

response. The set point is changed to 14 degree again after the first 500 seconds, and kept there for additional 500 seconds. Experimental data is sampled each second, and the data is evaluated for 1000 seconds in total.

Fig. 12 and 13 show swing disturbance response of PI control with/without DFC. The PI control received the effects of the load disturbance, and then the superheat controller cannot regulate the set point around 10 degree. On the other hand, the proposed method can track the set point even though the load change disturbed the regulation. The suction pressure control for compressor with DFC gets worse slightly, however both controllers can keep the set point 2.5 ± 0.15 [bar] and maintain the stability.

Table 6 shows IAE of the superheat control and suction pressure control with/without DFC. IAE of the suction pressure control gets worse by 18.12. On the other hand, superheat control with DFC obtained IAE=640.23 and improved 52.43 % compared to only PI control (IAE=1345.80).

5. DISCUSSION AND CONCLUSIONS

This paper presents MIMO robust Disturbance Feedback Control using an LMI approach. The experimental results of the refrigeration system demonstrated the robustness of the proposed DFC. As future work, we will consider input constraints for this method, and we may also examine fixed order DFC design.

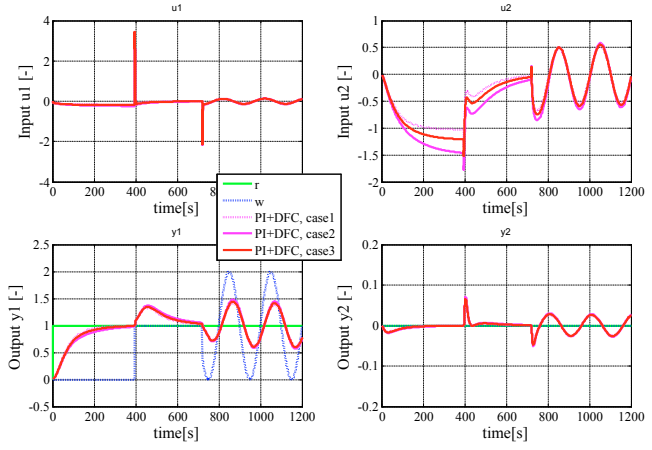

Fig. 10. Simulation results using PI control with full order DFC.

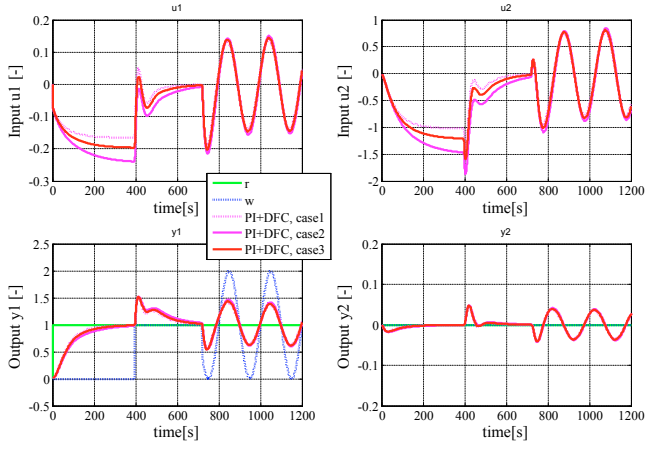

Fig. 11. Simulation results using PI control with DFC gain.

ACKNOWLEDGMENT

The authors wish to thank the anonymous reviewers for constructive comments.

REFERENCES

Åström, K. and Hägglund, T. (2005). *Advanced PID Control. 2005, The Instrumentation, Systems, and Automation Society*. Research Triangle Park, NC 27709.

Boyd, S., Hast, M., and Åström, K.J. (2015). MIMO PID Tuning via Iterated LMI Restriction. *International Journal of Robust and Nonlinear Control, DOI: 10.1002/rnc.3376*.

Carsten Scherer and Siep Weiland (2004). Linear matrix inequalities in control. URL `http://www.dcsc.tudelft.nl/~cscherer/lmi/notes05.pdf`.

Chilali, M., Gahinet, P., and Apkarian, P. (1999). Robust pole placement in LMI regions . *IEEE Transactions on Automatic Control*, 44(12), 2257 – 2270.

Cottle, R.W. (1974). Manifestations of the Schur complement. *Linear Algebra and its Applications*, 8(3), 189–211.

Gahinet, P.M. and Apkarian, P. (1994). A Linear Matrix Inequality Approach to H_∞ Control. *International Journal of Robust and Nonlinear Control*, 4(4), 421–448.

Ge, M., Chiu, M.S., and Wang, Q.G. (2002). Robust PID controller design via LMI approach. *Journal of Process Control*, 12(1), 3–13.

Hoshino, T., Itoh, J.I., and Kaneko, T. (2007). Dead-time voltage error correction with parallel disturbance observers for high performance v/f control. In *Proc. Industry Applications Conference*, 2038 – 2044. New Orleans, LA.

Izadi-Zamanabadi, R., Vinther, K., Mojallali, H., Rasmussen, H., and Stoustrup, J. (2012). Evaporator unit as a benchmark for plug and play and fault tolerant control. In *Proc. 8th IFAC Symposium on Fault Detection, Supervision and Safety of Technical Processes*, 701–706. Mexico City, Mexico.

Kawai, F., Vinther, K., Andersen, P., and Bendtsen, J.D. (2015). Pid control with robust disturbance feedback control. In *The 2015 IEEE Multi-Conference on Systems and Control (MSC);*, 1223–1229. Sydney.

Michael Grant and Stephen Boyd (2014). CVX: Matlab software for disciplined convex programming, version 2.1, build 1107. URL `http://cvxr.com/cvx`.

Table 5. Experimental conditions.

Set point	Value	Controlled by
Superheat	10.0 [C]	PI + DFC
Suction pressure	2.5 [bar]	PI + DFC
Condenser	9.0 [bar]	PI
Water tank	14.0 [C]	PI

Table 6. IAE of the experimental results.

	PI	PI + DFC (gain)
The superheat control	1345.80	640.23
The suction pressure control	26.89	45.01

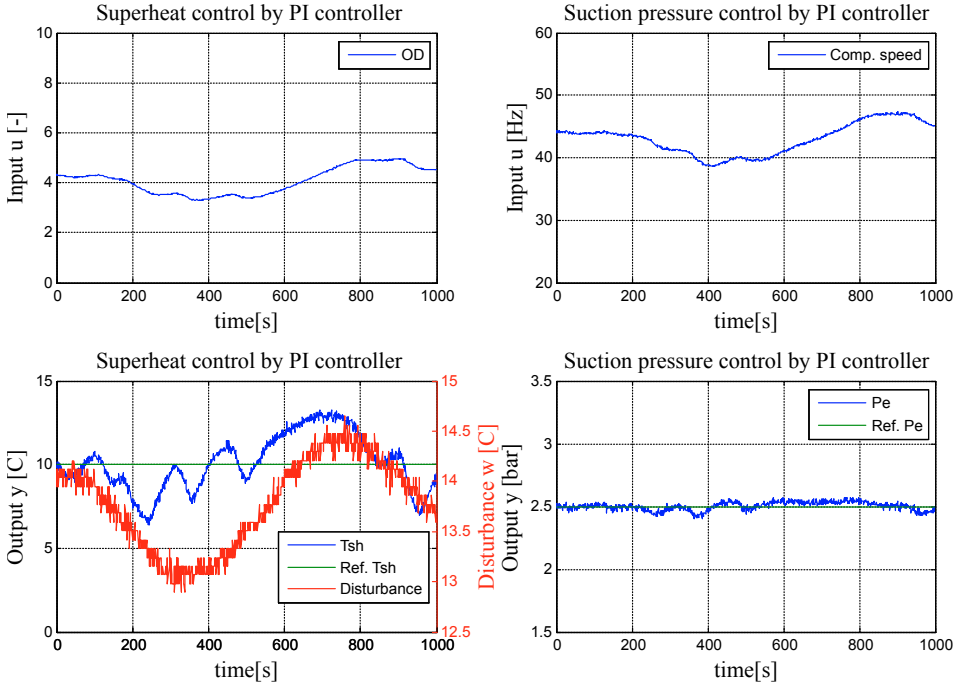

Fig. 12. Swing disturbance response with PI control without DFC gain.

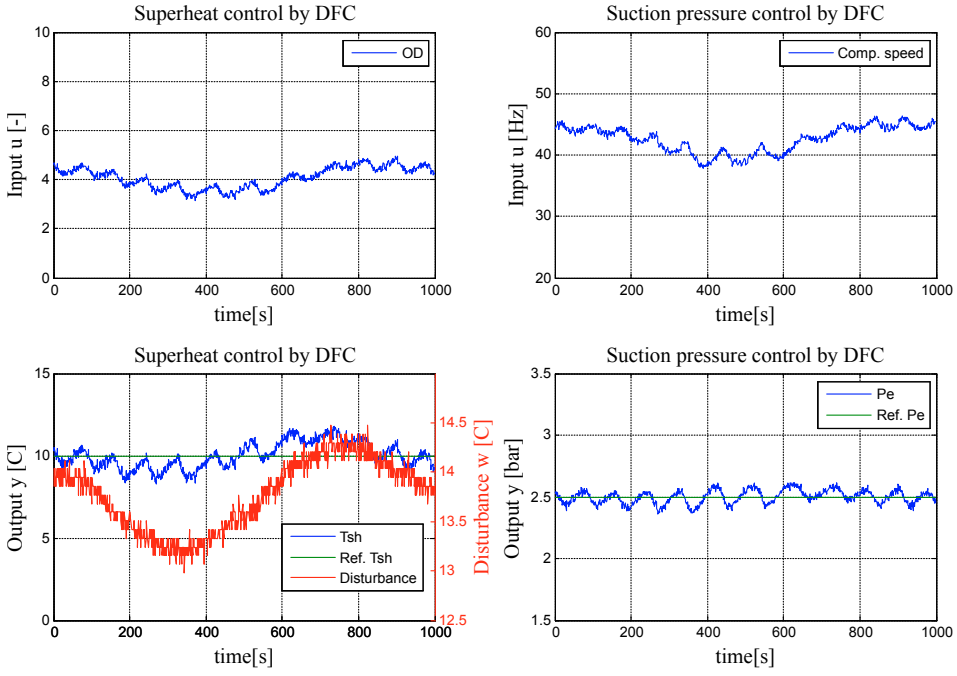

Fig. 13. Swing disturbance response with PI control with DFC gain.

Ohishi, K., Ohnishi, K., and Miyachi, K. (1983). Torque - speed regulation of dc motor based on load torque estimation method. In *Proc. International Power Electronics Conference (IPEC)*, 1209 – 1218. Tokyo.

Sadabadi, M. and Karimi, A. (2013). An lmi formulation of fixed-order h infinity and h2 controller design for discrete-time systems with polytopic uncertainty. In *Proc. Decision and Control (CDC), 2013 IEEE 52nd Annual Conference*, 2453 – 2458. Firenze.

Scherer, C., Gahinet, P., and Chilali, M. (1997). Multiobjective Output-Feedback Control via LMI Optimization. *IEEE Transactions on Automatic Control*, 42(7), 896–911.

Sivrioglu, S. and Nonami, K. (1996). Lmi approach to gain scheduled h_∞ control beyond pid control for gyroscopic rotor-magnetic bearing system. In *Proc. Decision and Control (CDC), 1996 IEEE 35th Annual Conference*, 3694–3699. Kobe, Japan.